NMR Spectroscopy

DOI: 10.1002/anie.201105984

Solid-State NMR Spectroscopy on Cellular Preparations Enhanced by Dynamic Nuclear Polarization**

*Marie Renault, Shane Pawsey, Martine P. Bos, Eline J. Koers, Deepak Nand, Ria Tommassen-van Boxtel, Melanie Rosay, Jan Tommassen, Werner E. Maas, and Marc Baldus**

Solid-state NMR (ssNMR) spectroscopy offers increasing possibilities to study complex biomolecules at the atomic level.[1] An important target area concerns membrane-associated proteins, which can be investigated by ssNMR methods after reconstitution in synthetic bilayers. While such preparations allow examination of functional aspects of the protein of interest, the influence of the native cellular environment on protein structure and function cannot be monitored. Very recently, we introduced a general approach aimed at determining complex molecular structures, including integral membrane proteins, in their native cellular environment by ssNMR under magic-angle-spinning (MAS) conditions.[2,3] Using dedicated sample-preparation routes, we demonstrated that high-resolution ssNMR spectra can be obtained on uniformly ^{13}C,^{15}N-labeled preparations of *Escherichia coli* whole cells (WC) and cell envelopes (CE). Both CE and WC morphology are preserved under standard ssNMR experimental conditions and the corresponding ^{13}C and ^{15}N cross-polarization (CP-MAS) spectra are invariant over time. However, with increasing levels of molecular complexity, especially in the case of WC preparations, spectroscopic sensitivity becomes a critical factor.

In recent years, dynamic nuclear polarization (DNP) has developed into a routine tool to increase the sensitivity of multidimensional ssNMR.[4] DNP enhancements of up to 148-fold have been obtained on micro/nanocrystalline biomolecular samples, including an amyloidogenic peptide and a deuterated protein,[5,6] while enhancements between 18- and 46-fold have been reported for membrane-embedded polypeptides, purple membrane preparations, and bacteriophages.[7,8] Here, we investigated the use of DNP to conduct ssNMR studies on ^{13}C,^{15}N-labeled preparations of *E. coli* WC overproducing the integral outer membrane protein PagL.[9] In Figure 1, we compared ^{13}C and ^{15}N CP-MAS spectra of uniformly ^{13}C,^{15}N-labeled WC with the CE isolated from PagL-overproducing *E. coli* cells, recorded in the presence and absence of microwave irradiation. At higher temperatures (271 K), ssNMR spectra of the *E. coli* CE had previously revealed atomic details of PagL as well as endogenous membrane-associated macromolecules, including the major lipoprotein Lpp and non-proteinaceous components such as lipopolysaccharides (LPS), peptidoglycans (PG), and phospholipids.[3] Under low-temperature (LT) DNP conditions, we observed significant DNP enhancement factors for both preparations in spectral regions characteristic for protein signals (aliphatic ^{13}C resonances: $\delta = 50$–55 ppm, amide ^{15}N backbone and side-chain resonances at about 120 and 80–30 ppm) as well as for ^{13}C signals of endogenous

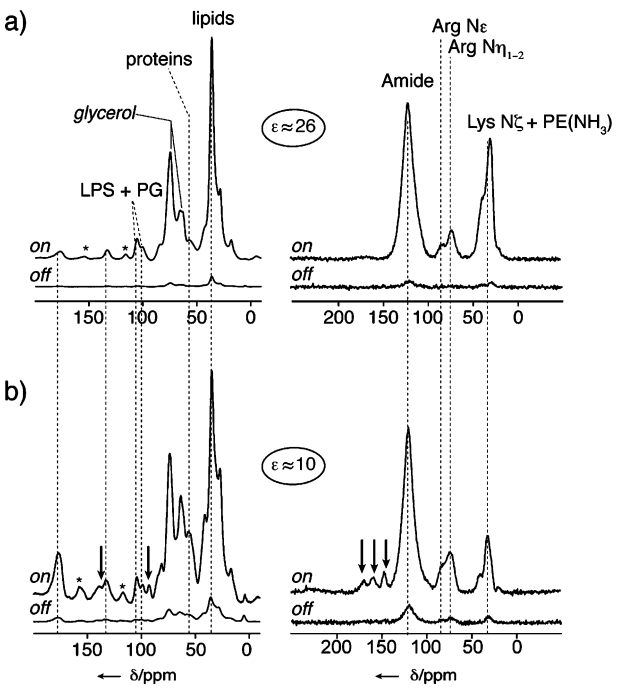

Figure 1. Comparison of ^{13}C (left) and ^{15}N (right) CP-MAS spectra of (U-^{13}C,^{15}N)-labeled CE (a) and WC (b) with (top trace, "on") and without (bottom trace, "off") DNP, using a microwave irradiation time of 10 s. Significant differences in the spectra of the two preparations are denoted by arrows. Asterisks indicate MAS side bands. Assignments of major *E. coli* molecular components are, if available, annotated and signal enhancements are given. Natural abundance ^{13}C signals from glycerol ($\delta^{13}C \approx 73$ and 63 ppm) present in the glassy matrix and from the silicon plug ($\delta^{13}C \approx 4$ ppm) are visible in the ^{13}C CP spectra of the WC and CE preparations.

[*] Dr. M. Renault, E. J. Koers, Dr. D. Nand, Prof. M. Baldus
Bijvoet Center for Biomolecular Research, Utrecht University
Padualaan 8, 3584 CH Utrecht (The Netherlands)
E-mail: m.baldus@uu.nl
Dr. M. P. Bos, R. Tommassen-van Boxtel, Prof. J. Tommassen
Department of Molecular Microbiology, Utrecht University
Padualaan 8, 3584 CH Utrecht (The Netherlands)
Dr. S. Pawsey, Dr. M. Rosay, Dr. W. E. Maas
Bruker BioSpin Corp., Billerica, MA 01821 (USA)

[**] This study was presented in part at the 52nd ENC conference, Asilomar, CA, April 10–15, 2011. Funding by NWO (grants 700.26.121 and 815.02.012) and the European Community's Seventh Framework Program [FP7/2007-2013] under Grant Agreement no. 211800 is gratefully acknowledged.

Supporting information for this article is available on the WWW under http://dx.doi.org/10.1002/anie.201105984.

phospholipids, PG, and LPS resonating at approximately 34, 92–103, and 95–104 ppm, respectively.

A similar DNP enhancement was found for glycerol peaks ($\delta^{13}C \approx 63$ and 73 ppm) constituting the glassy matrix. The latter signals were efficiently suppressed in dipolar (^{13}C,^{13}C) double-quantum (Figure S1 in the Supporting Information) and 2D (^{15}N-^{13}C) (Figure S2 in the Supporting Information) correlation spectra which confirmed the presence of major endogenous membrane-associated macromolecules, specifically LPS, PG and phosphatidylethanolamine (PE). Furthermore, we observed a set of new signals in the WC spectra resonating at $\delta = 92$ ppm and 138.4 ppm in the ^{13}C CP spectrum and 146.0 ppm, 158.5 ppm and 169.7 ppm in the ^{15}N CP spectrum (arrows in Figure 1b).

To understand the nature of these signals, we conducted a series of 2D heteronuclear ssNMR experiments on the uniformly ^{13}C,^{15}N-labeled WC preparation. As shown in Figure 2a, the 2D (^{1}H,^{15}N) heteronuclear correlation spectrum revealed intense correlations between ^{15}N signals resonating at $\delta = 158.5$ and 148.0 ppm and ^{1}H resonance frequencies between 10.5 and 14.5 ppm, characteristic of imino signals of nucleotides (BMRB; Biological Magnetic Resonance Data Bank, http://www.bmrb.wisc.edu/).

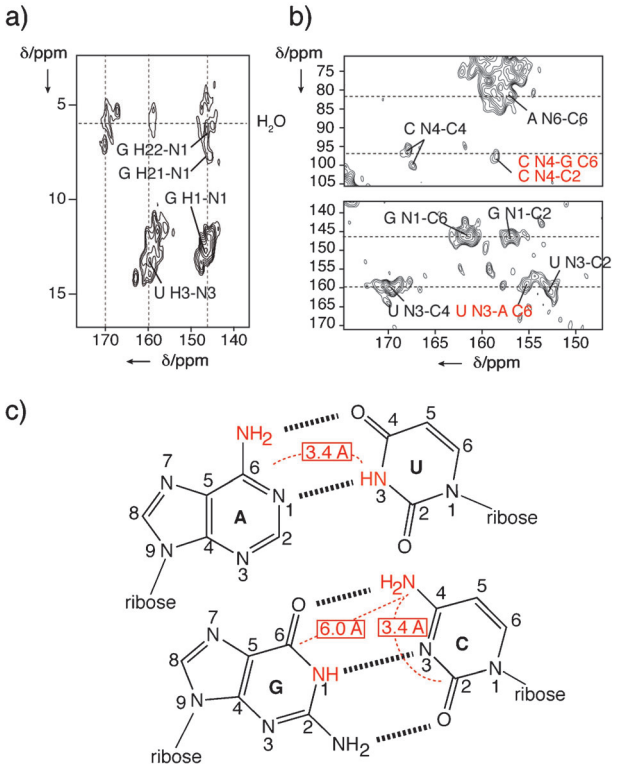

Figure 2. Selected regions from DNP-enhanced a) 2D (^{1}H,^{15}N) FSLG HETCOR and b) 2D (^{15}N,^{13}C) NCO spectra obtained on (U-^{13}C,^{15}N)-labeled WC showing characteristic correlations of RNAs. Indicated assignments are based on BMRB average chemical shifts from common RNA nucleotides. c) Chemical structure of standard RNA bases with Watson–Crick base-pairing throughout. Intra- and intermolecular contacts between cytosine N4 or uracil N3 and other C atoms that support our assignment are indicated.

The presence of nucleic acid derived signals in the spectrum was corroborated by the observation of well-resolved N–C correlations between imino ^{15}N resonances and ^{13}C signals resonating between $\delta = 170$ and 153 ppm in the 2D NCO spectrum (Figure 2b), and consistent with one-bond N^{H}–C' contacts within guanine and uracil nucleotides. In addition, we observed a set of additional isolated correlations in the same ^{13}C frequency range, involving ^{15}N resonances at $\delta \approx 95$ ppm, in good agreement with averaged chemical shift of cytosine N4. According to standard nucleotide-specific peak positions and the overall dispersion of N–C correlations, ^{15}N signals in the spectral regions of $\delta = 80$–100 and 145–165 ppm of the ^{15}N CP-MAS WC spectrum predominantly reflect nucleic acid resonances. Indeed, WC were collected from uniformly ^{13}C,^{15}N-labeled cultures after 4 h of induction with isopropyl-β-D-thiogalactopyranoside (IPTG) before the cells entered the stationary growth phase. Under these conditions, RNA accounts for roughly 21 wt% of *E. coli* macromolecules whereas DNA is 10 times less abundant.[10] Assuming a standard A-form helical stem portion of RNA with Watson–Crick base-pairing throughout, we could assign several of the detected correlations to intra- and/or intermolecular contacts between protonated nitrogen and other C atoms of RNA bases (Figure 2c). Additional correlations of lower intensity were observed between the water ^{1}H resonance at $\delta = 6$ ppm and uracil N3/guanine N1 indicating that a subset of imino groups from RNA molecules are water exposed.

Finally, we investigated whether the overexpressed integral membrane protein PagL could be characterized in a whole-cell setting. We hence recorded a set of 2D NCA correlation spectra in which signals from non-proteinaceous molecular components are drastically reduced. A DNP-enhanced 2D NCA spectrum obtained on a WC preparation (Figure S3 in the Supporting Information) revealed correlations typical for folded proteins, with well-dispersed glycine signals (region I) and N–Cα correlations typical of α-helical protein segments (region II). To assist our spectroscopic analysis, we compared our results with ssNMR data obtained at higher temperature (271 K) on CE preparations and purified PagL-containing proteoliposomes (PL) (Figure 3). In region I (Figure 3, upper row), Gly correlations seen in both CE isolated from PagL-overexpressing cells (blue) and in PL (red) are in good agreement with the cross-peak pattern of a DNP-enhanced NCA correlation spectrum of WC (black). Such correlations are absent in ssNMR spectra of CE prepared from non-induced cells (upper row, left), suggesting that the strongest signal sets in these spectra must stem from endogenous molecular components that are largely devoid of glycine residues.

In region II (Figure 3, lower row), ssNMR correlations are largely absent in proteoliposome preparations (red). Indeed, this spectroscopic region should predominantly contain NCA–protein correlations in α-helical or, to a smaller extent, random-coil conformations in line with only a single Thr34 correlation of the β-barrel protein PagL in proteoliposomes shown in Figure 3. In contrast, the peak pattern seen in the WC sample overlaps with correlations seen in CE preparations isolated from non-induced (green) and IPTG-induced (blue) WC and can be readily attributed to the

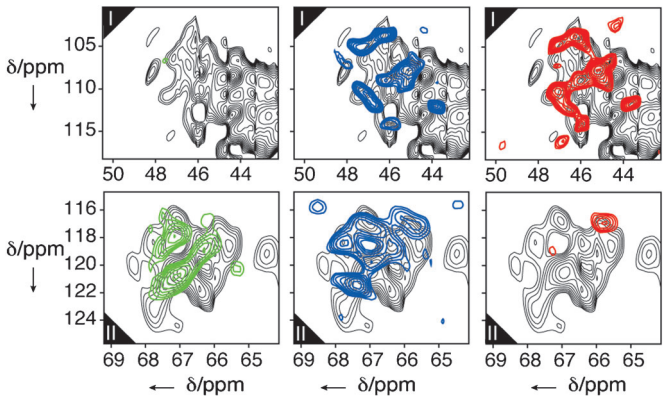

Figure 3. Overlay of the DNP-enhanced 2D (^{15}N,^{13}C) NCA correlation spectra of (U-^{13}C,^{15}N)-labeled WC (at 100 K, 8 kHz MAS) (black) and the 2D NCA of (U-^{13}C,^{15}N)-labeled CE isolated from noninduced (green) or PagL-overexpressing (blue) cells and purified (U-^{13}C,^{15}N)-PagL reconstituted in proteoliposomes (red) obtained at 271 K and 13 kHz MAS). Upper row: region I, lower row: region II.

lipoprotein Lpp, which belongs to the most abundant CE-associated proteins in exponentially growing cells and lacks Gly in its amino acid sequence.[3] Thus, regions I and II in Figure 3 strongly suggest that both PagL (I) as well as endogenous Lpp (II) can be detected in WC preparations under DNP conditions. Notably, with an average ^{13}C linewidth of $\delta = 0.8$–0.9 ppm, the low-temperature ssNMR spectra compared favorably to ssNMR spectra recorded at 271 K.

Taken together, these results show that DNP can be readily combined with ssNMR approaches in cells. Our results suggest that the application of LT-DNP not only increases spectroscopic sensitivity by at least an order of magnitude but also permits the detection of molecular components that are not associated with specific compartments. Compared to standard ssNMR spectroscopy, DNP at low temperatures and the use of free radicals can complicate sample preparation and can potentially give rise to reduced spectral resolution. However, using the preparations described herein, our spectra are of comparable resolution to those obtained in previous studies at higher temperature. ssNMR spectroscopy in cells as described here hence permits the tracking of entire cellular compartments similar to cryo-electron tomography but further work will be needed to conduct such experiments under in vivo conditions. Initial studies in our laboratory suggest that low temperatures and cryo-protection with 15–40% glycerol are beneficial for WC sample stability and viability. In our experiments, ^{13}C and ^{15}N signal enhancements are similar in magnitude to those in previous studies that used TOTAPOL as a radical in (protonated) purple-membrane preparations or bTbK on peptides in deuterated POPC bilayers.[8,7] Typical *E. coli* cell dimensions of $0.5\,\mu m \times 2\,\mu m$ are comparable to those in earlier successful DNP studies on amyloid nanocrystals.[5] Our study revealed that both CE-associated molecular components, including integral membrane proteins, lipoproteins, lipids, and periplasmic PG, and cytoplasmic macromolecules such as nucleic acids are readily visible. Unlike the case of the crystals, solute *E. coli* particles and solvent molecules were enhanced by a similar factor. Further signal enhancements should be possible by optimization of the sample preparation procedures including molecular deuteration and the choice of the radical. DNP-enhanced ssNMR spectroscopy as shown here provides a novel approach to study diverse cellular components and their involvement in fundamental biological processes ranging from molecular signal transduction to protein (mis)folding,[11] at atomic resolution with exquisite sensitivity.

Experimental Section

Uniformly ^{13}C,^{15}N-labeled preparations of *E. coli* whole cells (WC), cell envelopes (CE), and PagL-containing proteoliposomes (PL) were obtained by following the procedure described elsewhere.[3] Pellets of exponentially growing WC were washed three times in a $H_2O/D_2O/[D_8]$glycerol matrix (10/30/60 wt%) containing 60 mM TOTAPOL by resuspension/centrifugation cycles at 4000 *g*.[12] The CE were placed in the same matrix with 60 mM TOTAPOL and pelleted at 95000 *g*. WC and CE samples were subsequently transferred into 3.2 mm Bruker sapphire rotors with a (silicon) top spacer using a tabletop centrifuge ($14000 \times g$). Samples were precooled at $-20\,^{\circ}C$ prior to DNP ssNMR measurements. DNP experiments were performed on a Bruker 263 GHz Solids DNP spectrometer, consisting of a 263 GHz continuous-wave gyrotron source, microwave transmission line, 3.2 mm low-temperature MAS probe, gas cooling supply, and 400 MHz AVANCE III wide-bore NMR system.[13] NMR spectra were processed using Topspin 3.0 (Bruker BioSpin, Germany) and analyzed with Sparky.[14] ^{13}C and ^{1}H resonances were calibrated using adamantane as an external reference, and ^{15}N chemical shifts were referenced indirectly to liquid ammonia.[15,16] Further information about ssNMR experimental parameters is given in the Supporting Information.

Received: August 24, 2011
Revised: November 2, 2011
Published online: February 1, 2012

Keywords: analytical methods · dynamic nuclear polarization · membrane proteins · RNA · solid-state NMR spectroscopy

[1] a) E. Brunner, C. Groger, K. Lutz, P. Richthammer, K. Spinde, M. Sumper, *Appl. Microbiol. Biotechnol.* **2009**, *84*, 607–616; b) C. Wasmer, L. Benkemoun, R. Sabate, M. O. Steinmetz, B. Coulary-Salin, L. Wang, R. Riek, S. J. Saupe, B. H. Meier, *Angew. Chem.* **2009**, *121*, 4952–4954; *Angew. Chem. Int. Ed.* **2009**, *48*, 4858–4860; c) M. Renault, A. Cukkemane, M. Baldus, *Angew. Chem.* **2010**, *122*, 8524–8535; *Angew. Chem. Int. Ed.* **2010**, *49*, 8346–8357.

[2] E. R. Andrew, A. Bradbury, R. G. Eades, *Nature* **1958**, *182*, 1659.

[3] M. Renault, R. Tommassen-van Boxtel, M. P. Bos, J. A. Post, J. Tommassen, M. Baldus, *Proc. Natl. Acad. Sci. USA* **2012**, in press.

[4] a) A. B. Barnes, G. D. Paepe, P. C. van der Wel, K. N. Hu, C. G. Joo, V. S. Bajaj, M. L. Mak-Jurkauskas, J. R. Sirigiri, J. Herzfeld, R. J. Temkin, R. G. Griffin, *Appl. Magn. Reson.* **2008**, *34*, 237–263; b) T. R. Carver, C. P. Slichter, *Phys. Rev.* **1956**, *102*, 975–980; c) A. Lesage, M. Lelli, D. Gajan, M. A. Caporini, V. Vitzthum, P. Mieville, J. Alauzun, A. Roussey, C. Thieuleux, A. Mehdi, G. Bodenhausen, C. Coperet, L. Emsley, *J. Am. Chem. Soc.* **2010**, *132*, 15459–15461; d) T. Maly, G. T. Debelouchina, V. S. Bajaj, K. N. Hu, C. G. Joo, M. L. Mak-Jurkauskas, J. R. Sirigiri, P. C. van der Wel, J. Herzfeld, R. J. Temkin, R. G. Griffin, *J. Chem. Phys.* **2008**, *128*, 052211.

[5] P. C. van der Wel, K. N. Hu, J. Lewandowski, R. G. Griffin, *J. Am. Chem. Soc.* **2006**, *128*, 10840 – 10846.
[6] U. Akbey, W. T. Franks, A. Linden, S. Lange, R. G. Griffin, B. J. van Rossum, H. Oschkinat, *Angew. Chem.* **2010**, *122*, 7971 – 7974; *Angew. Chem. Int. Ed.* **2010**, *49*, 7803 – 7806.
[7] E. Salnikov, M. Rosay, S. Pawsey, O. Ouari, P. Tordo, B. Bechinger, *J. Am. Chem. Soc.* **2010**, *132*, 5940 – 5941.
[8] a) M. L. Mak-Jurkauskas, V. S. Bajaj, M. K. Hornstein, M. Belenky, R. G. Griffin, J. Herzfeld, *Proc. Natl. Acad. Sci. USA* **2008**, *105*, 883 – 888; b) M. Rosay, A. C. Zeri, N. S. Astrof, S. J. Opella, J. Herzfeld, R. G. Griffin, *J. Am. Chem. Soc.* **2001**, *123*, 1010 – 1011; c) V. S. Bajaj, M. L. Mak-Jurkauskas, M. Belenky, J. Herzfeld, R. G. Griffin, *J. Magn. Reson.* **2010**, *202*, 9 – 13.
[9] L. Rutten, J. Geurtsen, W. Lambert, J. J. Smolenaers, A. M. Bonvin, A. de Haan, P. van der Ley, M. R. Egmond, P. Gros, J. Tommassen, *Proc. Natl. Acad. Sci. USA* **2006**, *103*, 7071 – 7076.
[10] F. C. Neidhardt in *Escherichia coli and Salmonella: Cellular and Molecular Biology*, *Vol. 1*, 2nd ed. (Eds.: R. Curtiss III, J. L. Ingraham, E. C. C. Lin, K. Brooks Low, B. Magasanik, W. S. Reznikoff, M. Riley, M. Schaechter, H. E. Umbarger), ASM, Washington, **1996**, pp. 13 – 16.
[11] M. Renault, M. P. Bos, J. Tommassen, M. Baldus, *J. Am. Chem. Soc.* **2011**, *133*, 4175 – 4177.
[12] C. Song, K. N. Hu, C. G. Joo, T. M. Swager, R. G. Griffin, *J. Am. Chem. Soc.* **2006**, *128*, 11385 – 11390.
[13] M. Rosay, L. Tometich, S. Pawsey, R. Bader, R. Schauwecker, M. Blank, P. M. Borchard, S. R. Cauffman, K. L. Felch, R. T. Weber, R. J. Temkin, R. G. Griffin, W. E. Maas, *Phys. Chem. Chem. Phys.* **2010**, *12*, 5850 – 5860.
[14] T. D. Goddard, D. G. Kneller, *SPARKY 3*, University of California, San Francisco.
[15] C. R. Morcombe, K. W. Zilm, *J. Magn. Reson.* **2003**, *162*, 479 – 486.
[16] a) J. L. Markley, A. Bax, Y. Arata, C. W. Hilbers, R. Kaptein, B. D. Sykes, P. E. Wright, K. Wuthrich, *J. Mol. Biol.* **1998**, *280*, 933 – 952; b) R. K. Harris, E. D. Becker, S. M. Cabral de Menezes, R. Goodfellow, P. Granger, *Solid State Nucl. Magn. Reson.* **2002**, *22*, 458 – 483.

